Supplementary Data

Supplementary Methods

Proliferation analysis

3-(4,5-dimethylthiazol-2-yl)-2,5-diphenyltetrazolium bromide (MTT) colorimetric assay was utilized for assessing cell proliferation by measuring the activity of enzymes that reduce MTT or close dyes to formazan dyes, giving a purple color. The analysis was performed according to manufacturer's protocol (Vybrant®; Molecular Probes, Inc.). The actual number of viable cells was also counted utilizing Trypan Blue staining (0.8 m*M* in phosphate-buffered saline).

Melanoma cell culture

Primary melanoma wm3211 cells were cultured in RPMI1640 with 10% fetal bovine serum (FBS), penicillin (100 units/ml)/streptomycin (0.1 mg/ml), and 0.01 mg/ml insulin. Human metastatic melanoma cell line Lu1205 was cultured in L15/MCDB medium with 10% FBS and penicillin/streptomycin. Human metastatic melanoma A375 (American Type Culture Collection, ATCC), SK-Mel28 (ATCC), c83-2c, c81-61, and c81-46A cells (established by our lab from melanoma patients) were cultured in Dulbecco's Modified Eagle Medium (DMEM) or F10 medium, respectively—each supplied with 5% FBS, 5% new born bovine serum, and penicillin and streptomycin (3).

Ultraviolet radiation and cell treatment

Cells were grown to about 70% confluence and the medium was removed completely for ultraviolet (UV) radiation. For UVA radiation, 5 ml of PBS was added to one 10-cm dish of cells and ice cubes were placed next to dishes for absorbing the heat generated by UVA. UVA or UVB radiation was performed in a Stratagen crosslinker with peak wavelength at 350 or 312 nm, respectively. The UV intensity was measured by a radiometer with proper probes. A fresh medium was added back after radiation and cells were returned to 37°C incubator for recovery. For drug treatments, neuronal nitric oxide synthase (nNOS) inhibitors or resveratrol or curcumin were added into the culture medium either 24 h before radiation or right after radiation when adding a fresh medium.

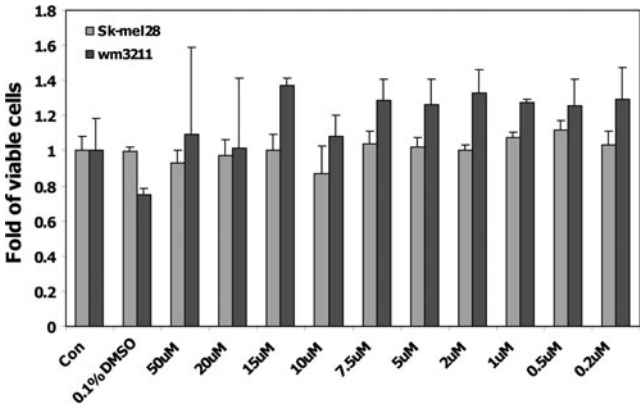

SUPPLEMENTARY FIG. S1. Effects of neuronal nitric oxide synthase inhibitor JI-16 on cell proliferation in human melanoma cells. MTT colorimetric assay was employed after 72 h of treatments, and the relative proliferation rate was represented as fold of control cells.

K_i *value calculation*

Recombinant nitric oxide synthase isozymes overexpressed in *E. coli* were utilized (1,2). Relative enzyme inhibition activity [%] versus Log (inhibitor concentration [M]) correlation was analyzed by Prism using nonlinear regression method to generate IC_{50} value. The K_i value was calculated by $IC_{50} = K_i(1 + [S]/K_m)$.

Adhesion analysis of human metastatic melanoma A375 cells to fibroblast cells

A375 cells were added to the fibroblast cell monolayer (FB) and incubated with the presence or absence of nNOS

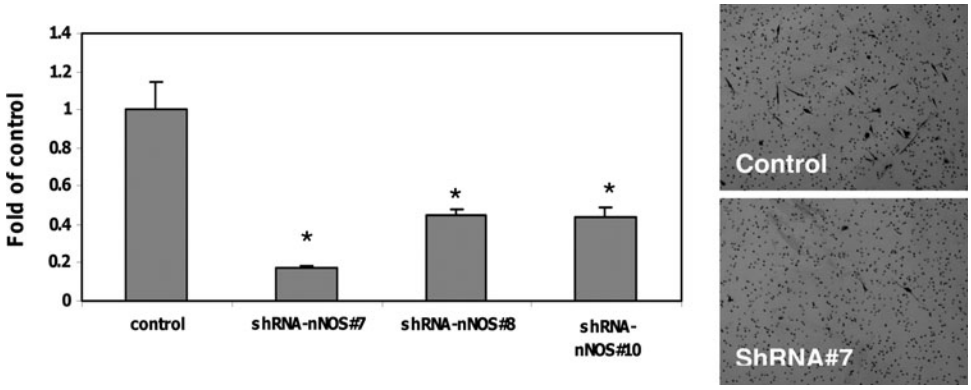

SUPPLEMENTARY FIG. S2. Stable knockdown of neuronal nitric oxide synthase (nNOS) significantly reduced the invasion potential of human melanoma Lu1205 cells. shRNA-nNOS#7, shRNA-nNOS#8, and shRNA-nNOS#10 represent different cells overexpressing distinct nNOS shRNA constructs. Control represents Lu1205 cells stably integrating control shRNA construct.

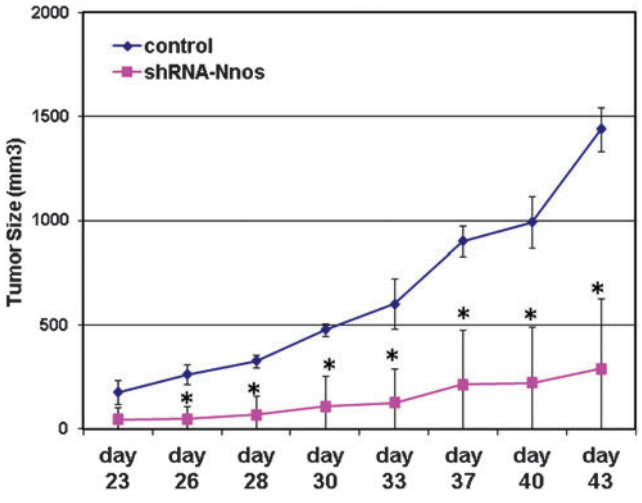

SUPPLEMENTARY FIG. S3. Effects of nNOS knockdown on tumor growth of human melanoma Lu1205 cells in a xenograft mouse model. About 1×10^6 Lu1205 cells were injected to nude mouse subcutaneously on blank. The growth of tumor was measured three times a week. Tumor volume was calculated as follows: tumor volume (mm^3) = (length/2) × (width)^2. *$p < 0.05$ compared to control ones that were injected with Lu1205 cells carrying shRNA-control construct.

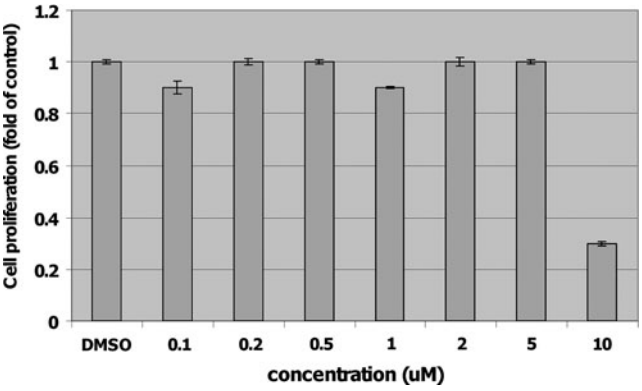

SUPPLEMENTARY FIG. S4. Effects of cpd2 on cell proliferation in human immortalized human melanocytes. Cells were treated with different concentrations of cpd2 for 72 h, followed by MTT colorimetric analysis.

inhibitors (2 μM) for 1 h. Nonadhesive cells were washed away by PBS and MTT reagent was utilized to determine the relative amount of cells that adhered to FB cells, which is calculated as fold of control representing the relative effects of compounds on melanoma adhesion.

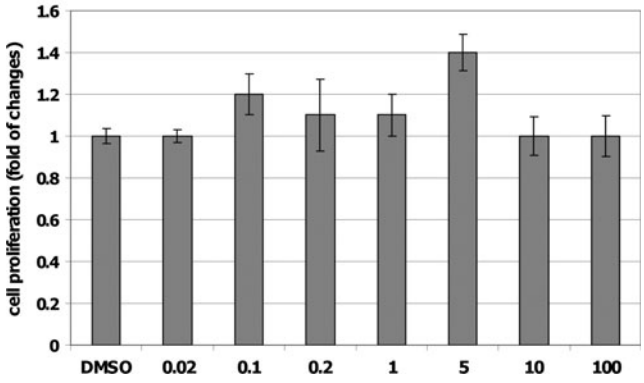

SUPPLEMENTARY FIG. S5. No significant cytotoxicities occurred after treatments of inducible NOS inhibitor aminoguanidine in human melanoma wm3211 cells up to 100 μM.

Ultrasensitive colorimetric NOS activity analysis

Employing a NADPH recycling system, the analysis kit allows NOS to operate linearly for hours as NO-derived nitrate and nitrite accumulate, and enables efficient high-throughout screening of NOS activity in resting cells or cell lysates as well as biological fluids and tissue homogenates. In addition, this kit can be used to accurately measure as little as 1 pmol/μl ($\sim$1 μM) NO produced in aqueous solutions (1–100 μM).

Results

Novel synthesized nNOS inhibitor JI-16 is the same as cpd2 except that the phenyl group is absent. In contrast to cpd2, which exhibited promising antimelanoma activities, our MTT colorimetric assay showed that up to 50 μM, JI-16 did not exhibit any inhibitory effects on melanoma cell proliferation after a 3-day treatment.

As shown in Supplementary Figure S2, stable knockdown of nNOS significantly reduced the invasion potential of human metastatic Lu1205 cells. ShRNA-nNOS#7, shRNA-nNOS#8, and shRNA-nNOS#10 represent different cells overexpressing distinct nNOS shRNA constructs. Among them, the inhibition by shRNA-nNOS#7 was most potent.

Consistent with our *in vivo* study utilizing A375 melanoma cells, stable knockdown of nNOS (by shRNA-nNOS#7) in another metastatic melanoma cell line Lu1205 also significantly inhibited tumor growth in xenograft mouse model (Supplementary Fig. S3). The average of measured tumor size (mm^3) is much smaller compared to that of the control group ($p < 0.05$). Notable, in contrast to A375, the tumor growth of Lu1205 is much slower.

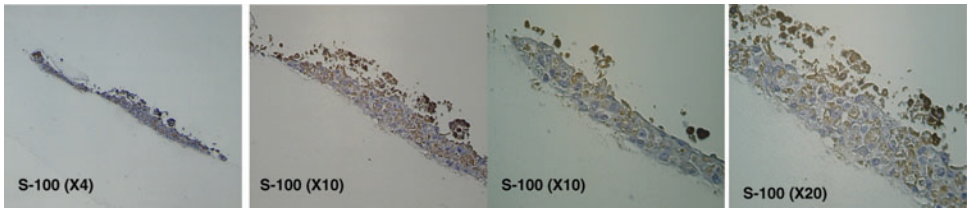

SUPPLEMENTARY FIG. S6. Melanoma lesions grown in three-dimensional skin reconstructs were confirmed by S-100 positive staining (brown).

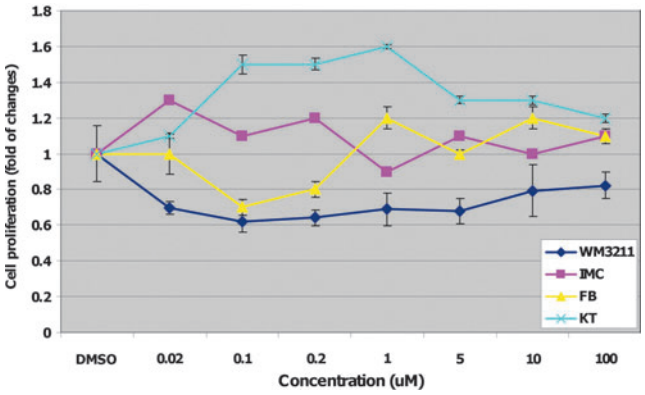

SUPPLEMENTARY FIG. S7. No significant cytotoxities were evident in human immortalized melanocytes, fibroblast cells, and keratinocytes treated with cpd8 for 72 h, while cpd8 reduced cell proliferation of primary melanoma wm3211 cells. MTT colorimetric assay was employed after 72 h of treatments, and the relative proliferation rate was represented as fold of control cells.

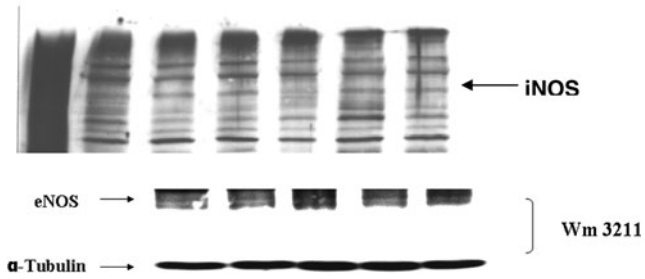

SUPPLEMENTARY FIG. S8. Effects of iNOS and eNOS expression levels after ultraviolet A (UVA) radiation. Same amounts of samples as used in Figure 2E were subjected for immunoblotting analysis and the expression levels of iNOS and eNOS were detected by specific antibodies. These are the images of prolonged exposure (>5 min).

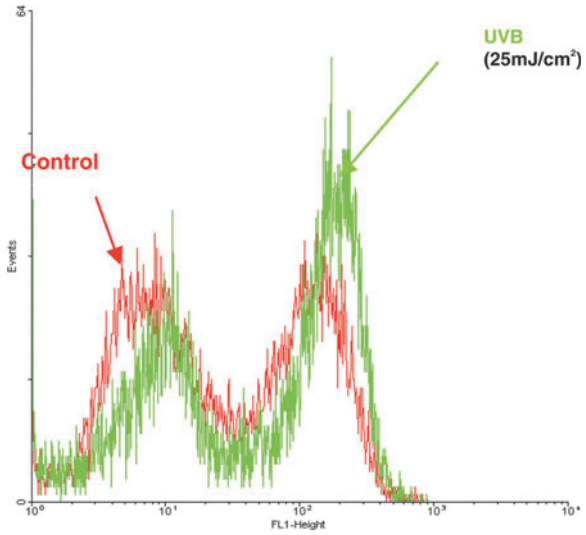

SUPPLEMENTARY FIG. S9. Induction of intracellular NO levels after UVB radiation detected by fluorescence probe DAF-FM (4-amino-5-methylamino- 2′,7′-difluorofluorescein) and flow cytometry. Two hours later after UVB radiation, cells were labeled by DAF-FM (10 μM) for 30 min. Single-cell suspensions were collected for flow cytometry analysis.

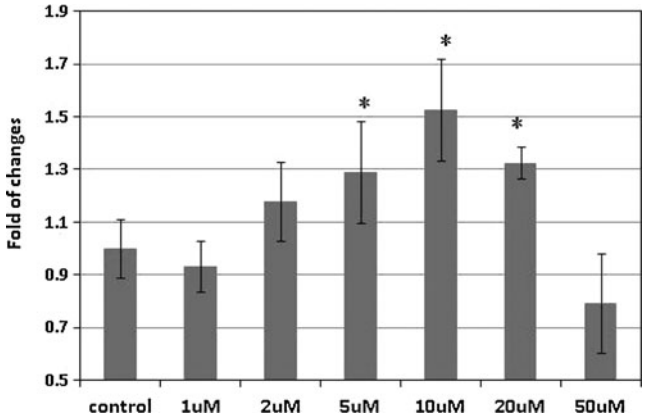

SUPPLEMENTARY FIG. S10. Effects of (*Z*)-1-[2-(2-aminoethyl)-*N*-(2-ammonioethyl) amino] diazen-1-ium-1,2-diolate on proliferation of human melanoma A375 cells. MTT colorimetric assay was employed after 72 h of treatments, and the relative proliferation rate was represented as fold of control cells. *$p < 0.05$ compared to control.

Due to the very slow proliferation rate of normal human melanocytes and the impracticality of using them for screening studies, we used immortalized human melanocytes instead for the assay of cpd2 cytotoxicity. In contrast to the promising cytotoxicites occurred in melanoma cells, cpd2 up to 5 μM exhibited no significant toxicities in immortalized melanocytes even after 72 h of exposure (Supplementary Fig. S4).

Cell proliferation analysis showed that commercially available inducible NOS (iNOS) inhibitor aminoguanidine exhibited no significant cytotoxic effects on human melanoma wm3211 cells up to 100 μM after 3 days of treatment (Supplementary Fig. S5).

As shown in Supplementary Figure S6, the melanoma lesions grown in three-dimensional skin constructs were confirmed by S-100 immunohistochemistry staining. The brown stainings represent the presences of melanoma cells.

cpd8 exhibited no cytotoxic effect on human primary fibroblast cells, keratinocytes, and immortalized melanocytes up to 100 μM, while it did inhibit cell proliferation of primary melanoma wm3211 cells (Supplementary Fig. S7). Such inhibition, however, was not in a typical dose-dependent manner. At 1 μM, cpd8 reduced the cell proliferation to 69% of control.

As shown in our Supplementary Data (Supplementary Fig. S8), the expression levels of iNOS and endothelial NOS were much lower compared to nNOS. iNOS might also contribute to the increase of NO generation after UV radiation, but compared to nNOS, its effects are limited to a much lesser extent.

We also measured intracellular nitric oxide (NO) levels utilizing fluorescence probe DAF-FM (4-amino-5-methylamino- 2′,7′-difluorofluorescein) detected by flow cytometry according to manufacturer's protocol (Molecular Probes, Life Technologies) (Supplementary Fig. S9). Consistently, after 2 h of UVB radiation (25 mJ/cm^2), fluorescence density was increased compared to control cells.

As shown in our Supplementary Data (Supplementary Fig. S10), the stimulation of proliferation by DETA/NO treatment reached a peak at 10 μM, which was, however, reversed by a higher concentration of DETA (50 μM). Our data are

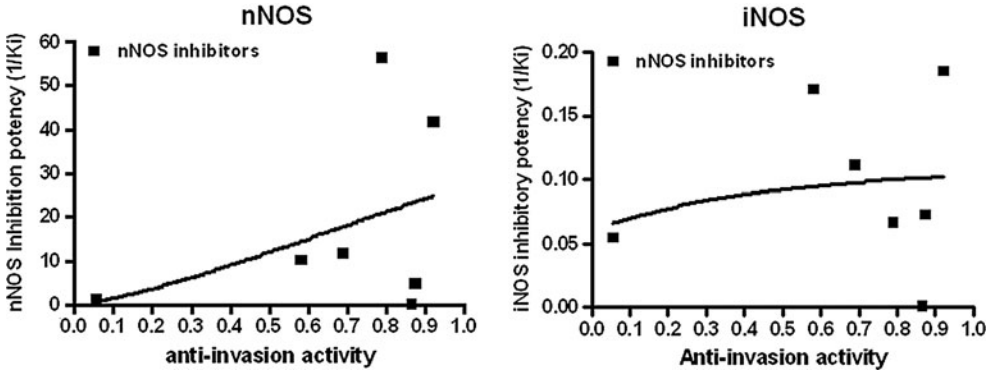

SUPPLEMENTARY FIG. S11. Correlation analysis of novel nNOS inhibitors between anti-invasion activity and nNOS or iNOS inhibition potency (represented as $1/K_i$). Linear regression analysis was performed utilizing SAS statistic software.

consistent with other researchers' studies, suggesting that, in human melanoma, lower level of NO is more proliferative while higher level of NO is proapoptotic.

To determine whether the inhibitions of nNOS correlated with their anti-invasive activities, we employed linear regression analysis utilizing SAS statistic software (Supplementary Fig. S11). Our correlation analysis of anti-invasion potential and iNOS inhibitory potency [represented as $1/K_i$(iNOS)] has produced an R^2 of 0.0153 ($p=0.7917$) and for nNOS inhibition potency [represented as $1/K_i$(nNOS)], an R^2 value of 0.1467 ($p=0.3964$) was obtained. No significant correlation was detected by our analysis.

As shown in Supplementary Figure S12, we performed actual counting of viable cells after distinct treatments utilizing Trypan Blue staining in different cell lines. Consistent with our MTT data (Fig. 1B), we observed a stimulating effect of NO stress on cell proliferation generated by (*Z*)-1-[2-(2-aminoethyl)-*N*-(2-ammonioethyl) amino] diazen-1-ium-1,2-diolate (DETA/NO) and L-arginine with marked increase of viable cell numbers. Notably, in immortalized melanocytes,

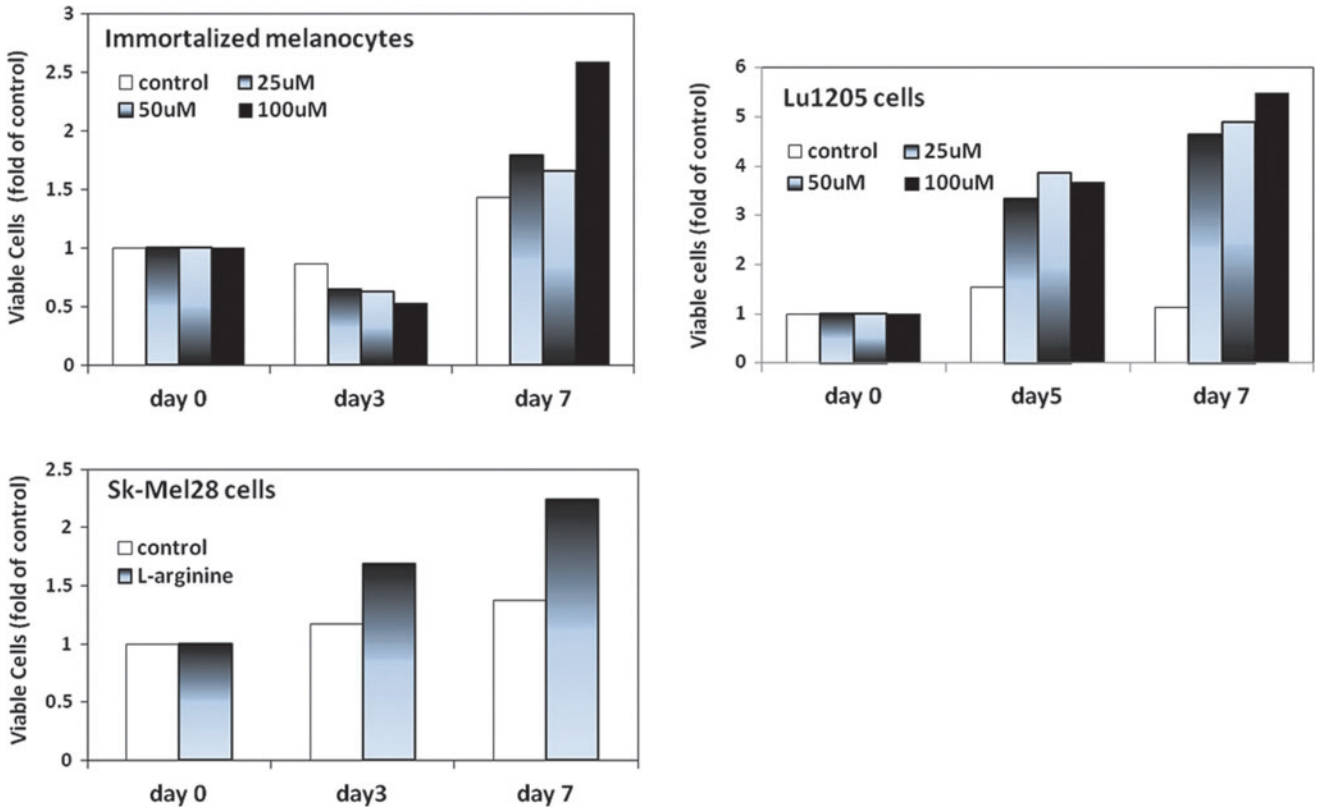

SUPPLEMENTARY FIG. S12. NO stress generated by (*Z*)-1-[2-(2-aminoethyl)-*N*-(2-ammonioethyl) amino] diazen-1-ium-1,2-diolate (DETA/NO) or L-arginine stimulated cell proliferation in immortalized melanocytes, metastatic melanoma Lu1205 and Sk-Mel28 cells. The actual number of viable cells was counted by Trypan Blue staining and normalized by the number on day 0. The concentration of L-arginine was 2.87 m*M*.

such stimulation by DETA/NO was only evident after 7 days of treatment.

References

1. Ji H, Delker SL, Li H, Martasek P, Roman LJ, Poulos TL, and Silverman RB. Exploration of the active site of neuronal nitric oxide synthase by the design and synthesis of pyrrolidinomethyl 2-aminopyridine derivatives. *J Med Chem* 53: 7804–7824, 2010.
2. Ji H, Li H, Martasek P, Roman LJ, Poulos TL, and Silverman RB. Discovery of highly potent and selective inhibitors of neuronal nitric oxide synthase by fragment hopping. *J Med Chem* 52: 779–797, 2009.
3. Yang S, Irani K, Heffron SE, Jurnak F, and Meyskens FL. Alterations in the expression of the apurinic/apyrimidinic endonuclease-1/redox factor-1 (APE/Ref-1) in human melanoma and identification of the therapeutic potential of resveratrol as an APE/Ref-1 inhibitor. *Mol Cancer Ther* 4: 1923–1935, 2005.